

## Identification of Strong and Weak Interacting Two-Level Systems in KBr:CN

Alejandro Gaita-Ariño<sup>1</sup> and Moshe Schechter<sup>2</sup>

<sup>1</sup>*Department of Physics & Astronomy, University of British Columbia, Vancouver, B.C., Canada, V6T 1Z1*

<sup>2</sup>*Department of Physics, Ben Gurion University - Beer Sheva 84105, Israel*

(Received 26 November 2010; revised manuscript received 17 May 2011; published 2 September 2011)

Tunneling two-level systems (TLSs) are believed to be the source of phenomena such as the universal low temperature properties in disordered and amorphous solids, and  $1/f$  noise. The existence of these phenomena in a large variety of dissimilar physical systems testifies for the universal nature of the TLSs, which however, is not yet known. Following a recent suggestion that attributes the low temperature TLSs to inversion pairs [M. Schechter and P. C. E. Stamp, [arXiv:0910.1283](https://arxiv.org/abs/0910.1283).] we calculate explicitly the TLS-phonon coupling of inversion symmetric and asymmetric TLSs in a given disordered crystal. Our work (a) estimates parameters that support the theory in M. Schechter and P. C. E. Stamp, [arXiv:0910.1283](https://arxiv.org/abs/0910.1283), in its general form, and (b) positively identifies, for the first time, the relevant TLSs in a given system.

DOI: [10.1103/PhysRevLett.107.105504](https://doi.org/10.1103/PhysRevLett.107.105504)

PACS numbers: 63.20.kp, 61.43.Fs, 63.20.kk, 65.60.+a

*Introduction.*—Amorphous solids and many disordered lattices show peculiar universal characteristics at low temperatures [1–3]. Below  $T_U \approx 3$  K systems which are otherwise very different have specific heat  $C_v \propto T^\alpha$ , with  $\alpha \approx 1$ , thermal conductivity  $\kappa \propto T^\beta$  with  $\beta \approx 2$ , and internal friction  $Q \approx 2\pi l/\lambda \approx 10^3$ , independent of  $T$ ,  $\lambda$ , and with only a small variance between materials. Here  $l$  is the phonon mean free path and  $\lambda$  is the phonon wavelength. In an effort to explain this remarkable universality, Anderson, Halperin, and Varma [4], and Philips [5] suggested a phenomenological theory, where the existence of tunneling two-level systems (TLSs) in these materials was postulated, and an ansatz for their density of states was given. This “standard tunneling model” (STM) has been very successful in explaining the above mentioned phenomena. Still, the identity of the tunneling TLSs has remained unknown. Furthermore, the smallness and universality of the phonon attenuation, and the energy scale dictating  $T_U$  are not accounted for by the STM.

Two-level systems are also believed to be the cause of  $1/f$  noise. Recently, it has been shown that  $1/f$  noise is the main source for decoherence of superconducting qubits, and a major obstacle in their ability to perform quantum computation [6]. Also in these systems the nature of the TLSs is not known, yet assuming their existence and applying the STM has resulted in an explanation of the low frequency  $1/f$  noise and high frequency linear in  $f$  noise on the same footing [7].

Extensive experimental investigations have revealed that the condition to observe universality is the presence of tunneling states and strong lattice strain [8,9], and that the phenomena in amorphous solids and disordered crystals are equivalent [10]. Disordered crystals are advantageous for both experimental and theoretical investigation [11]. Experimentally, they allow control of the nature and relative concentration of host material and impurities, and therefore a detailed study of different universal properties

and their origin. The existence of lattice structure and the apparent candidates for tunneling states allows a favorable starting point for theoretical treatment as well.

Indeed, it was argued [12] that, at least in disordered crystals, tunneling states can be categorized into two types of TLSs, denoted  $\tau$  and  $S$ . The states of a  $\tau$  TLS are related to each other by inversion. Consequently, the interaction of a  $\tau$  TLS with the phonon field  $\gamma_w$  is small, as it results only from disorder induced local deviations from inversion symmetry. The  $S$  TLSs are asymmetric with respect to local inversion, with a strong interaction with the phonon field  $\gamma_s$ . It was then shown [12] that the  $S$  TLSs are gapped below  $T_U$  by the  $\tau$  TLSs through an Efros-Shklovskii-type [13] mechanism, and that below  $T_U$  the  $\tau$  TLSs are effectively noninteracting, and dictate the phonon attenuation. Thus, at  $T < T_U$  the  $\tau$  TLSs fulfil the assumptions of the STM. The small parameter of the theory is  $g \equiv \gamma_w/\gamma_s \approx E_\phi/E_C \sim (1-3) \times 10^{-2}$ , where  $E_\phi$ ,  $E_C$  are the typical elastic and Coulomb energies in the system. This small parameter gives the universality and smallness of the phonon attenuation. Defining  $T_G$  as the ordering temperature of the  $S$  TLSs, the emerging DOS of the  $S$  TLSs at an energy  $T_U \approx gT_G$ , dictates  $T_U$  as the energy scale below which universality is observed [12].

In this Letter we use DFT and *ab-initio* calculations to calculate the interaction of TLSs of types  $\tau$  and  $S$  with the phonon field in the system  $\text{KBr}_{(1-x)}(\text{CN})_x$  (KBr:CN, Fig. 1). We find that  $\gamma_w \approx 0.1$  eV, and  $\gamma_s \approx 3$  eV. Our estimation of  $\gamma_w$  compares well with the experimentally measured value for the relevant TLSs at low energies, of  $\gamma \approx 0.12$  eV for impurity concentration  $x = 0.25$  and  $\gamma \approx 0.2$  eV for  $x = 0.5$  [14,15]. Our results also support the central arguments of the theory in Ref. [12] in (i) the categorization of the TLSs according to their symmetry under inversion, (ii) the ratio of the strengths of their interactions with the phonon field, constituting the small parameter of the theory, and (iii) the identification of the

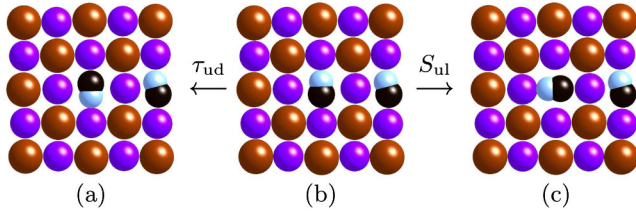


FIG. 1 (color online). Three  $5 \times 5$  fragments of a KBr:CN lattice. The *up* state of the central impurity in fragment (b) is related by a  $\tau$  excitation to a *down* state in fragment (a), and by an  $S$  excitation to a *left* state in fragment (c).

symmetric TLSs as the relevant TLSs dictating the low temperature universal properties in disordered solids. In addition, we reinforce the prediction made in Ref. [12] for the existence, at higher energies, of a second type of TLSs (of  $S$  type), with a much stronger coupling to the phonon field. Note, that although we focus here on the simplest single impurity excitations, our analysis does not exclude the possibility of symmetric and asymmetric multi-impurity excitations [16–18]. Such excitations are expected to be significant especially for systems where single impurity excitations do not produce symmetric TLSs [19,20].

For the specific KBr:CN system, early works have suggested, based on theories quite different from that of Ref. [12], that CN flips comprise the relevant low energy TLSs [21,22]. However, for long, advance in this direction was hindered because of experiments showing that the substitution of the symmetric  $N_2$  molecules for the asymmetric CO molecules in  $N_2$ :Ar:CO does not change its universal characteristics [19,20]. Our results here, in conjunction with the theory in Ref. [12], positively identify the  $180^\circ$  CN flips as the relevant TLS excitations dictating the low temperature characteristics in the KBr:CN system. Reconciliation of our results with the experiment in Refs. [19,20] stems from the fact that pairs of  $N_2$  molecules do produce symmetric TLSs in the  $ArN_2$  system [23].

*Calculation.*—KBr:CN is perhaps the most studied disordered lattice showing universal characteristics. The  $CN^-$  impurities have been found to orient either in the direction of the in-space diagonals, preferred for very low  $CN^-$  concentrations [24] and for intermediate concentrations at high temperatures [25], or in the direction of the axes, preferred for intermediate  $CN^-$  concentrations at low temperatures [25]. The six (eight) possible states of each impurity can be categorized into three (four) inversion pairs, each having two states related to each other by an  $180^\circ$  flip. Such flips constitute  $\tau$  excitations, whereas rotations between different axes (diagonals) correspond to  $S$  excitations [12,26].

The interaction of such a system with the lattice can be described by the Hamiltonian [12,26]

$$H_{\text{int}} = \sum_j \sum_{\alpha,\beta} [\eta \delta^{\alpha,\beta} + \gamma_s^{\alpha\beta} S_j^z + \gamma_w^{\alpha\beta} \tau_j^z] u_{\alpha\beta}(\mathbf{r}_j) \quad (1)$$

where  $\eta$  is an orientation-independent volume factor and  $u_{\alpha\beta}(\mathbf{r}_j)$  denotes the phonon field at point  $\mathbf{r}_j$ . Whereas the central purpose of this Letter is the calculation of  $\gamma_w$  and  $\gamma_s$ , we also calculate the parameter  $\eta$  for both  $CN^-$  and  $Cl^-$  impurities. This parameter determines the strain, and thus the effective random field in the system [26,27]. Usually  $\eta \lesssim \gamma_s$ . In KBr:CN  $\eta$  is significantly subdominant, as the  $Br^-$  and  $CN^-$  ions have similar volumes [15]. In KBr:Cl this term is responsible for the strains allowing for the existence of universal properties upon minimal  $CN^-$  dilution [8,9]. This random field term is also central to the smearing of the glass transition and the peculiar disordering of dilute glasses [27].

Following the above definition of  $\eta$ ,  $\gamma_s$  and  $\gamma_w$ , we devise a series of numerical calculations to estimate them. In sum, we choose a number of lattice fragments and use DFT–*ab initio* methods to calculate the energy difference between the effects of phononlike perturbations of the system with a central  $CN^-$  impurity in different states. For simplicity and without loss of generality, we restrict the excitations of the  $CN^-$  impurity under study to two dimensions, thus the possible states are *up*, *down*, *left* and *right*. To those possible orientations, we apply *vertical* or *horizontal* phonons. Usually the symmetry is low enough to allow for several independent estimations for each parameter.

Our determination of  $\gamma_w$  and  $\gamma_s$  is performed as follows:

$$\gamma_{w,s} = \frac{1}{b} |[E_{\text{ph}}^i(b) - E^i] - [E_{\text{ph}}^j(b) - E^j]| \quad (2)$$

where  $\{i, j\}$  are  $\{\text{up, down}\}$  or  $\{\text{left, right}\}$  for  $\gamma_w$  and  $\{\text{up, left}\}$  or  $\{\text{down, right}\}$  for  $\gamma_s$ , *ph* can stand for *vertical* or *horizontal* phonons,  $E^i$  is the energy of an impurity  $i$  surrounded by a lattice fragment in its equilibrium geometry and  $E_{\text{ph}}^i$  is the energy of the same impurity after a lattice contraction by a fraction  $b$  along a given crystallographic coordinate, mimicking the effect of a longitudinal phonon. For  $\eta$ , the same procedure is applied where  $\{i, j\}$  means presence or absence of impurity, and for  $CN^-$  impurities all possible orientations are averaged.

Figure 2 illustrates the detailed procedure of a  $\gamma$  calculation. We describe the position and orientation of the impurity as  $(2,0,u)$ , where the numbers refer to the coordinates and the letter to the orientation, in this case the  $CN^-$  is lying on the abscise, at 2 interatomic spacings to the right, and the nitrogen is pointing up. We then proceed with the following steps: (i) For that particular system, the atomic positions are found which minimize the energy in the absence of the TLS under investigation, i.e., when the central position is occupied by a  $Br^-$ ; that is our definition of the equilibrium geometry of the lattice. (ii) A  $CN^-$  (facing “up”, in this case) is substituted for the central  $Br^-$ , and, freezing the lattice, only the position of the  $CN^-$  is optimized, to obtain  $E^{\text{up}}$ . (iii) The atomic positions are contracted along the vertical axis to obtain  $E_{\text{vertical}}^{\text{up}}(b)$ . The

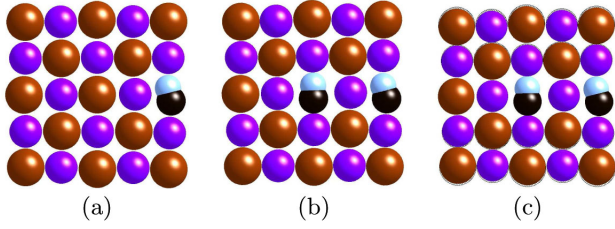


FIG. 2 (color online). Atomic coordinates of a lattice fragment in three key steps of a sample calculation. (a): all positions are optimized, without a central TLS, but in presence of an impurity (2,0,u). (b): a TLS (0,0,u) is substituted in the place of the central  $\text{Br}^-$ , its position is optimized, yielding  $E^i$ . (c): the lattice is contracted by 2% vertically, yielding  $E_{\text{vertical}}^i(-2\%)$ .

calculation is done for  $b \in \{-5\%, -2\%, -1\%, -0.25\%, 0.25\%, 1\%, 2\%, 5\%\}$ , and the limit of small  $b$  is taken (see Fig. 3). The repetition of this procedure for the vertical phonon and the “down,” “left,” and “right” orientations of the central  $\text{CN}^-$  allows for four nonindependent estimations of both  $\gamma_w$  and  $\gamma_s$  (in 3D we also have the “front” and “back” orientations). In the case of  $\eta$ , the weighted average for all orientations yields one unique estimation. Note that in step (ii) we do not relax the whole lattice in the presence of the TLS. Our procedure is in line with both processes of lattice relaxation and phonon scattering by TLSs, which result from the out of equilibrium first order interaction of the TLS with the lattice.

We use the standard package GAUSSIAN03 [28] to perform quantum chemistry calculations on lattice fragments of different sizes and shapes and at different levels of sophistication. As we are dealing with a local phenomenon, and for cost reasons, most of the calculations are

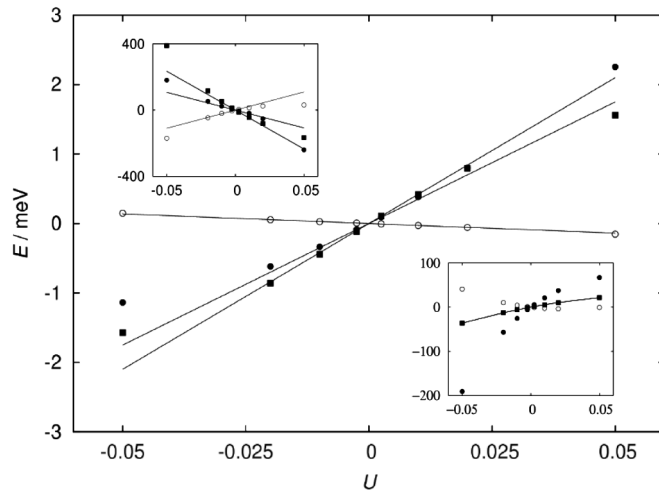


FIG. 3. Energy response  $E$  (in meV) to horizontal phonons of amplitude  $U$ .  $\gamma_w$  (main graph) and  $\gamma_s$  (upper inset) as linear fits on selected fragments on Table I: open circles: (b); filled circles: (c); squares: (d). Lower inset: second-order fit for  $\eta$  (see text); open circles:  $E_{\text{Br}} - E_{\text{up}}$ ; filled circles:  $E_{\text{Br}} - E_{\text{left}}$ ; squares: weighted average for all orientations.

performed on small zero-dimensional squares or cubes, either  $3 \times 3$ ,  $3 \times 3 \times 3$  or  $5 \times 5$ . The TLS under evaluation is always in the center, so that any deviation from a centrosymmetric situation felt by the TLS is due to the extra impurities and not to border effects. We mainly use the hybrid DFT–*ab initio* method B3LYP (three-parameter Becke–Lee–Yang–Parr functional) with small orbital sets, either 3-21G or 6-31G. The influence of a better description of the anions is tested by repeating some calculations with the more flexible basis sets, up to 6-311+G\*. Additionally, we check the relevance of dynamical correlation by comparing plain Hartree-Fock with the Moeller-Plesset perturbation theory to the second order (MP2), which includes double excitations as second-order perturbations. Last, we include a limited study of larger samples with a higher number of impurities, using HFS calculations with the minimal basis STO-3G on a  $7 \times 7$  fragment with up to 4 extra impurities.

**Results.**—Figure 3 illustrates some tests of the range of linearity. One can see that the results are essentially the same for different fragments and levels of calculations: the first order approximation is very accurate at least for phonon amplitudes of 1% or 2% of the interatomic spacing. On a  $3 \times 3$  fragment with a central  $\text{CN}^-$  impurity, at MP2–6-31+G level, Fig. 3 shows the estimation of  $\eta = 0.6$  eV. The same conditions yield a comparable  $\eta = 0.9$  eV for a  $\text{Cl}^-$  impurity. In all cases a noticeable second-order correction of the order of 5 eV can be fitted.

The central result of this Letter, reported in Table I, is the calculation of  $\gamma_s \approx 3$  eV and  $0 \leq \gamma_w \leq 0.15$  eV. The finite size of our samples, the quality of our calculation methods, and differences between planar and cubic samples, all lead to some variance in the parameters. Yet, the strength of our results lies in the fact that our estimations are fairly consistent in their order of magnitude for very different lattice fragments and a variety of levels of calculation. This is true for additional calculations, e.g., for a noncentral  $\text{CN}^-$  impurity, not reported here. The calculations using a minimal basis set serve to discard a correlation between  $\gamma_w$  or  $\gamma_s$  and the number of impurities.

One should point out that within a given sample and a given level of calculation, the variance in the values of  $\gamma_s$  between different orientations is a result of the small elastic deviations from symmetry, and are therefore a factor of  $g$  smaller than its typical value. With regard to  $\gamma_w$ , its values are dictated by the aforementioned deviation from local inversion symmetry. Thus, the distribution of all possible estimations of its values is peaked at zero, with a variance which equals the typical value. This is displayed in Table II, for all TLSs in fragment (a). It can also be seen in the main panel of Fig. 3, where the particular  $\tau$  TLS chosen for fragment (b) experiences a very symmetric environment. Note that for each particular combination of fragment and calculation method, the highest  $\gamma_w$  values obtained among the four TLS-phonon combinations are

TABLE I. Some estimations, in eV, for  $\gamma_s$  and  $\gamma_w$ . Absolute values are given, since the TLS orientation is arbitrary. Except for fragments (b)–(d), all possible TLSs were calculated, as shown for fragment (a) in Table II, and only the highest values are displayed here. In the absence of extra impurities,  $\gamma_w = 0$  for symmetry reasons. For fragments (b)–(d), only one  $\tau$  TLS and one  $S$  TLS were chosen, and linearity of the energy response was tested as shown in Fig. 3. For these fragments the values for  $\gamma_w$  should be considered as lower bounds. tr.ph. stands for “transverse phonon.” Fragment (e) sums up three calculations with a minimal basis set, with up to four impurities at positions  $(0, -2, r)$ ,  $(-2, 2, r)$ ,  $(2, 0, u)$ ,  $(2, 2, d)$ ; these results should not be taken on equal footing with the rest of the table.

Fragment	Impurity	Method	$\gamma_s$	$\gamma_w$
$3 \times 3$	None	HF-6-311+G*	3.02	0 (sym)
$3 \times 3$	None	MP2-3-21G	1.91	0 (sym)
$3 \times 3$	None	MP2-6-311+G*	3.55	0 (sym)
$3 \times 3$	None	B3LYP-3-21G	3.28	0 (sym)
$3 \times 3$ (tr.ph.)	None	B3LYP-3-21G	2.95	0 (sym)
$3 \times 3 \times 3$	None	B3LYP-3-21G	4.20	0 (sym)
$3 \times 3$ (tilt)	(1,1,dr)	B3LYP-6-31G	3.40	0.08
$3 \times 3^{(a)}$	(1,-1,dl)(1,1,ul)	B3LYP-3-21G	2.86	0.03
$3 \times 3^{(b)}$	(1,-1,dr)(1,1,ul)	MP2-6-311G	1.80	0.003
$3 \times 3 \times 3^{(c)}$	(0,-1,1,r)(1,-1,0,f)	HF-6-31+G	2.15	0.04
$3 \times 3 \times 3$ (tilt)	(1,1,dl)	B3LYP-3-21G	n.a.	0.14
$5 \times 5^{(d)}$	(0,-2,r)	B3LYP-6-31G	4.70	0.04
$5 \times 5$	(-1,-1,r)	B3LYP-3-21G	2.10	0.04
$5 \times 5$	(2,0,d)	B3LYP-3-21G	2.40	0.11
$7 \times 7^{(e)}$	(see caption)	HFS-STO-3G	10–20	0.1–0.2

denoted as our estimate values for  $\gamma_w$  in Table I. These values are the most relevant for our purposes, as they are expected to be the best predictors for a real system with many impurities.

A noteworthy complication is presented by the in-plane diagonal orientations of the TLS, because of the small energy difference with the in-space diagonal states in the real system. Depending on the fragment, impurities, and calculation method, the relative order of stability changes and the energy of one or more of the “axial” orientations rises above the most stable “diagonal” orientation. Some examples of these orientations, denoted as {dl, ul, dr, ur}, are shown in Table I. As illustrated in Figs. 1 and 2, in the perimeter of the fragment, where the  $\text{CN}^-$  suffer from intense border effects, we even find intermediate orientations. In the cases where the central TLS is affected by this problem—noted in Table I as “tilt”—the extraction of the parameters can be technically more difficult, but there is no fundamental physical difference between axial and

TABLE II. Values in eV, summary of results for fragment (a) on Table I. Shorthand  $\Delta_h^{\text{ud}} = (E_{\text{horizontal}}^{\text{up}} - E^{\text{up}}) - (E_{\text{horizontal}}^{\text{down}} - E^{\text{down}})$  has been used for clarity.

	$\gamma_s$		$\gamma_w$
$\Delta_h^{\text{ul}}$	2.84	$\Delta_h^{\text{ud}}$	0.0036
$\Delta_h^{\text{dr}}$	2.82	$\Delta_h^{\text{lr}}$	0.0070
$\Delta_v^{\text{ul}}$	<b>2.86</b>	$\Delta_v^{\text{ud}}$	0.0001
$\Delta_v^{\text{dr}}$	2.83	$\Delta_v^{\text{lr}}$	<b>0.0273</b>

diagonal orientations as in both cases there is a clear distinction between  $S$  TLSs and  $\tau$  TLSs.

*Summary.*—Our numerical calculations confirm qualitatively and quantitatively the results of Ref. [12]; the existence of weak and strong interacting TLSs in disordered solids, and the corresponding strength of their interaction with the phonon field. As TLSs in KBr:CN were experimentally measured to have a coupling constant of  $\gamma \approx 0.12 - 0.18$  eV with the phonon field, our calculations also verify that it is indeed the weak interacting  $\tau$  TLSs which are the relevant TLSs at low temperatures, dictating the universal behavior. Thus, we are able to clearly identify the relevant TLSs in this particular system. In Ref. [12] the plausibility that the same mechanism dictates universality in amorphous solids was argued for. The verification of this argument requires the identification of nearly inversion symmetric TLSs in amorphous solids, and the calculation of their coupling to the phonon field.

We would like to thank Ariel Amir, Lior Kronik, Juan José Serrano, José Sánchez-Marín, and Nicolas Suaud for useful discussions. A. G. A. acknowledges funding by call FP7-PEOPLE-2007-4-1-IOF, project PIOF-GA-2008-219514. M. S. acknowledges financial support from the ISF.

- [1] R. C. Zeller and R. O. Pohl, *Phys. Rev. B* **4**, 2029 (1971).
- [2] S. Hunklinger and A. K. Raychaudhuri, *Prog. Low Temp. Phys.* **9**, 265 (1986).

- [3] R. O. Pohl, X. Liu, and E. Thompson, *Rev. Mod. Phys.* **74**, 991 (2002).
- [4] P. W. Anderson, B. I. Halperin, and C. M. Varma, *Philos. Mag.* **25**, 1 (1972).
- [5] W. A. Phillips, *J. Low Temp. Phys.* **7**, 351 (1972).
- [6] R. W. Simmonds *et al.*, *Phys. Rev. Lett.* **93**, 077003 (2004).
- [7] A. Shnirman, G. Schon, I. Martin, and Y. Makhlin, *Phys. Rev. Lett.* **94**, 127002 (2005).
- [8] S. K. Watson, *Phys. Rev. Lett.* **75**, 1965 (1995).
- [9] K. A. Topp, E. J. Thompson, and R. O. Pohl, *Phys. Rev. B* **60**, 898 (1999).
- [10] X. Liu *et al.*, *Phys. Rev. Lett.* **81**, 3171 (1998).
- [11] R. O. Pohl, X. Liu, and R. S. Crandall, *Curr. Opin. Solid State Mater. Sci.* **4**, 281 (1999).
- [12] M. Schechter and P. C. E. Stamp, [arXiv:0910.1283](https://arxiv.org/abs/0910.1283).
- [13] A. L. Efros and B. I. Shklovskii, *J. Phys. C* **8**, L49 (1975).
- [14] J. F. Berret *et al.*, *Phys. Rev. Lett.* **55**, 2013 (1985).
- [15] J. J. De Yoreo, W. Knaak, M. Meissner, and R. O. Pohl, *Phys. Rev. B* **34**, 8828 (1986).
- [16] E. R. Grannan, M. Randeria, and J. P. Sethna, *Phys. Rev. B* **41**, 7784 (1990).
- [17] A. L. Burin, *J. Low Temp. Phys.* **100**, 309 (1995).
- [18] A. L. Burin and Yu. Kagan, *Phys. Lett. A* **215**, 191 (1996).
- [19] C. I. Nicholls, L. N. Yadon, D. G. Haase, and M. S. Conradi, *Phys. Rev. Lett.* **59**, 1317 (1987).
- [20] L. N. Yadon, C. I. Nicholls, and D. G. Haase, *Phys. Rev. B* **40**, 5215 (1989).
- [21] J. P. Sethna and K. S. Chow, *Phase Transit.* **5**, 317 (1985).
- [22] M. P. Solf and M. W. Klein, *Phys. Rev. B* **49**, 12703 (1994).
- [23] A. Gaita-Ariño, V. F. González-Albuixech, and M. Schechter (to be published).
- [24] H. U. Beyeler, *Phys. Rev. B* **11**, 3078 (1975).
- [25] A. Loidl, K. Knorr, J. M. Rowe, and G. J. McIntyre, *Phys. Rev. B* **37**, 389 (1988).
- [26] M. Schechter and P. C. E. Stamp, *J. Phys. Condens. Matter* **20**, 244136 (2008).
- [27] M. Schechter and P. C. E. Stamp, *Europhys. Lett.* **88**, 66002 (2009).
- [28] M. J. Frisch *et al.*, *Gaussian 03, Revision C.02* (Gaussian, Inc., Wallingford CT, 2004).